An Eye for Landscapes

Rapid Aerial Mapping with Handheld Sensors

This portable system offers fast deployment with no recalibration and maps both vertical and horizontal features while maintaining optimal flight parameters. The geo-referenced image and 3D point-cloud data can be processed into digital terrain models, digital surface models, and automatically derived 3D city models.

Jan Skaloud, Julien Vallet, Kristian Keller, Grégory Veyssière, and Otto Kölbl

Development of the HELIMAP system began in 1999 to address needs for natural hazards mapping and management. The main requirements were high resolution, accuracy, low cost, and portability. We have developed a portable mapping system that facilitates quick helicopter deployment, integrating high-accuracy GPS and inertial navigation sensors with an airborne laser scanner (ALS) and a high-resolution digital charge-coupled device (CCD) camera. Operated from the side of a helicopter, it produces high precision (about 0.1 meter), high resolution (up to 0.5 square meter) digital surface/terrain model (DSM/DTM) and orthorectified images (up to 0.05 meter/pixel).

These characteristics make the system suitable for applications such as:

- Environmental monitoring and natural hazards management: mapping and monitoring landslides, erosion, mud flows, cliffs, floods, glaciers, avalanches, and forestry
- Facility management: open-pit mines, powerlines, powerplants, transport infrastructure
- Corridor mapping: road and railway construction, powerline construction, rivers and hydrologic installations
- Civil aviation: obstacle mapping, approach and landing corridors, airport facility management
- Telecommunication: city models, planning of optimal antenna displacement
- Urban planning, tourism and GIS: 3D visualizations, fly-throughs, regional or heritage promotion, spatial planning

In most of these cases, the objects of interest are spread over a small area or narrow corridor(s). Others, such as those related to natural hazards, are of temporal or sporadic character that require mapping on short notice. Finally, several are vertically oriented (cliffs, landslides, and avalanches) and have important composition that is not

readily visible from above but rather from the side. These conditions make commercial mapping systems either too expensive or non-applicable, as their configuration is almost exclusively downward-looking, the installation time too long, and a stand-by mode not economically viable. HELIMAP enables quick deployment of the sensor block, operation in angles from nadir to horizon, and use without re-calibration between installations. Also, the use of smaller, off-the-shelf (OTS) sensors allows system amortization over projects of smaller size.

Natural hazards management includes all these challenges and the added demand to deliver fast mapping products to answer such questions as: How much snow has accumulated and how is it distributed? How much of the terrain has slid and where? Rescue services need correct information of this type to adequately manage, scale, and deploy their resources.

System Development

The first sensor was a high-quality analog camera that we later replaced with a high-resolution digital camera. The original integration of GPS and the inertial navigation system (INS) used a commercial solution. Later, internally developed hardware and software took over this function. Methods for rigorous system calibration were an important consideration.

Recently the system has been extended and is gaining interest for medium-range ALS (LiDAR) applications. New imagery and LiDAR sensors were implemented during winter 2004–2005, and the system integrates the latest in sensor technology and in sensor orientation and calibration. Universities, government agencies, and rescue services use HELIMAP data. The system can be modified from stand-by to operational mode quickly and easily.

System Design. The system concept incorporates a modular design with OTS sensors and modern communication to facilitate subsequent upgrades and part replacements. It is configured with moderately priced hardware and does not require a dedicated carrier. Its unique structure and mounting provide several advantages.

The lightweight carbon-aluminum structure joins GPS/INS/ALS and a high-resolution digital camera to a common sensor block that is 40×40×25 centimeters and weighs 12 kilograms. The block can be handheld or suspended on the side of a helicopter.

Installation time is minimal (less than 30 minutes) for fast deployment on short notice. Thanks to the sensor-head structure, no recalibration of spatial offsets or boresight is needed after the installation. We can perform oblique and nadir surveying with the same configuration and accuracy. As FIGURE 1 shows, we can eliminate the usual accuracy degradation due to the weak angle of incidence on steep surfaces by turning the sensor's head toward the slope. This is achieved either manually (with handheld installation) or during setup (in suspended installation).

The LiDAR and the digital camera have very similar fields of view, 60° and 56°, respectively, and the flying parameters of height and speed can be kept optimal simultaneously for both devices in most missions.

Sensor Head

The sensor head consists of navigation and remote-sensing devices, rigidly joined by a carbon-aluminum structure (FIGURE 2). The frame also incorporates the points of anchorage for safety cables and suspension and handles for manual steering. A manual camera trigger button is connected to one handle with a switch for accepting automatic trigger commands from a PC based on LiDAR and navigation data. The operator can override the automatic trigger using the manual trigger button.

The ALS is a short-range 2D scanner. The scanning angle is 60 degrees with a maximum range of 650 meters at 80 percent reflectance. Its rotating-mirror mechanism provides linear, unidirectional, and parallel scan lines with a programmable rate of up to 80 scans per second. The rate is chosen as a function of desired point density and flight parameters. Unlike most of today's airborne scanners, this instrument uses a short laser wavelength of 900 nanometers, ensuring favorable reflection even on snow-covered surfaces.

The system's digital camera has a focal length of 35 or 80 millimeters. The lens was chosen based on its high resolution, which was confirmed by field testing. Attached to the lens is a digital back. The hosted CCD chip has 5448×4080 pixels (22 megapixels) with 9-micrometer pixel

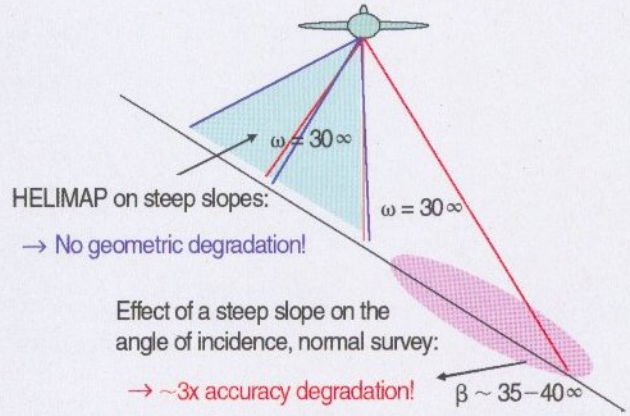

▲ **FIGURE 1** Steep slope looks flat as the system is kept perpendicular to the terrain all the way from nadir to horizon.

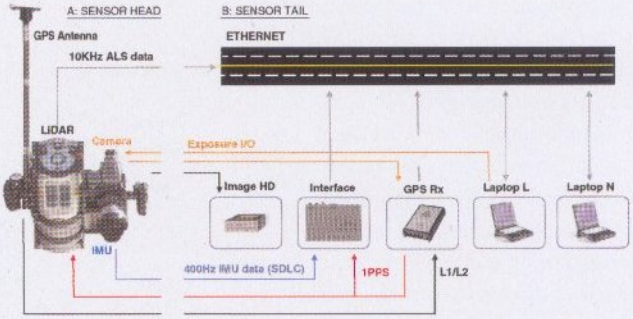

▲ **FIGURE 2** A) Image of compact sensor head, held or suspended outside helicopter. B) Schematic organization of sensor tail for data acquisition, synchronization, navigation, and instrument command.

▲ **HELIMAP SYSTEM** in nadir configuration for downward-looking data capture. It can also be configured to "map" laterally to better capture vertical surfaces.

size. The maximum image rate is shorter than two seconds. The shutter aperture generates a pulse that is interfaced via an X-sync bus of the camera to GPS event marker input.

The sensor head also incorporates a tactical grade inertial measurement unit (IMU) and a GPS-L1L2/GLONAS airborne antenna. The antenna is mounted on a carbon mast that can change orientation with respect to the LiDAR–camera plane from 15 to 90 degrees according to mapping requirements.

Sensor Tail

The sensor head is connected via cables to an infrastructure that ensures instrument maintenance, command, and data synchronization and storage. The communication spine of the system, shown in Figure 2, is an Ethernet that enables fast data exchange between the devices. The GPS, the LiDAR, and the computers are natural components of the Ethernet; the IMU is connected to this backbone via a specially designed interface that also synchronizes the incoming inertial data in the GPS time frame. Laptop N in Figure 2 is charged with GPS/INS data acquisition, interpretation, and flight management. Laptop L gathers the voluminous LiDAR data and controls the camera shutter in regard to flying speed, height above terrain, and a chosen overlap. The camera events are time-stamped by the bifrequency GPS receiver and communicated back to the flight management program. An external image bank stores as many as 850 pictures at full resolution. The Ethernet backbone enables standardized interfaces between individual elements and an open, modular design with replaceable OTS components. Finally, an uninterrupted power supply originally designed for the IMU and its interface was extended to supply power to the whole system. It ensures seamless switching between helicopter and 24 VDC battery power and conforms to instrument requirements.

Data Flow

FIGURE 3 depicts the coarse data flow from the sensors to the digital surface or terrain model (DSM/DTM) and the orthorectified image. The carrier-phase differential GPS positioning is integrated with inertial data in a loosely coupled configuration. This setup allows for the use of different software packages and suggests that a real-time version with thorough RT quality control is not far in the future. The laser range, amplitude, and encoder measurements are first interactively separated into individual flightlines. These data and the 400-Hz GPS/INS trajectory estimate are combined along with calibration information in the LiEO package to generate laser point clouds in the desired coordinate system. This output is further handled by a laser point clouds processing package for final surface and/or terrain model determination. This last step can be guided or potentially integrated by the image data.

The camera's exterior orientation (EO) parameters are calculated by the CamEO based on the same GPS/INS trajectory and appropriate calibration information. If rapid or less accurate products are needed, camera direct georeferencing (DG) is used together with the laser-determined DTM for orthophoto production. In the integrated sensor orientation scenario, assisted-automated aero-triangulation (AT) is introduced as an additional step for improved robustness and accuracy. The inclusion of GPS/INS-derived EO can substantially ease the process of automated tight-points generation, and this approach usually works well in a terrain of a favorable texture, such as outside the forest.

System Calibration

System calibration occurs in two major functions: lever arm and boresight. Lever arm is the spatial offsets between the origins of sensors for all possible GPS antenna positions (15° to 90° in 15° steps). It is determined with sub-centimeter accuracy in the laboratory by tachometric means.

Boresight is the term used for the an-

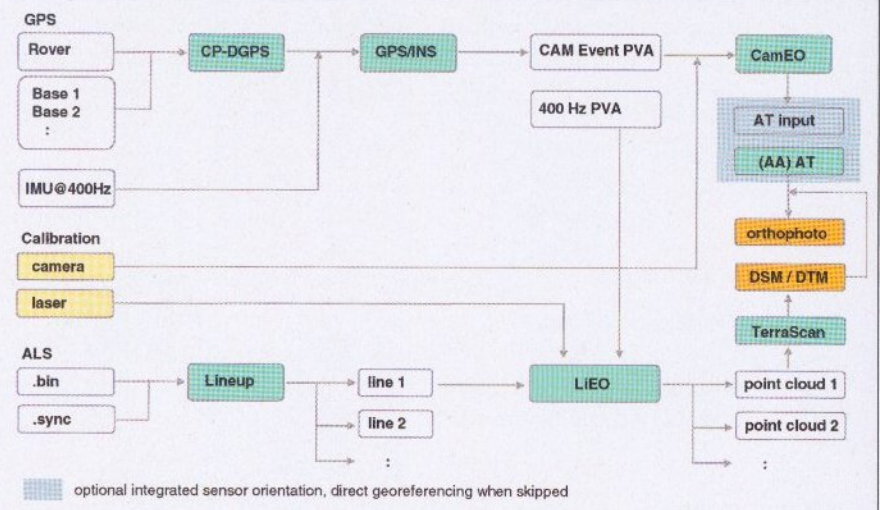

▲ **FIGURE 3** Direct georeferencing data flow for the orthophoto and DTM/DSM production

gular misalignment between the IMU and the CCD/LiDAR as a result of the mounting. The boresight with respect to the camera is determined with an accuracy better than 0.005°. The boresight determination with respect to LiDAR requires a special flying pattern over a selected terrain or feature. Beyond that, the ALS industry has adopted numerous ad hoc approaches with varying degrees of accuracy. We first tested a method using the slope gradients in DTM/DSM as it is implemented within software for correcting laser point-cloud data. The principal weakness of this approach is the strong correlation of the boresight angles with unknown terrain shape and the implemented stochastic model that assumes unrealistic time-invariant behavior of the GPS/INS errors. Later, we applied the cross-section method that is popular in commercial systems and usually provides satisfactory results for the boresight estimate in the roll direction; however, its use for the recovery of pitch and yaw/heading direction is less appropriate. We finally obtained satisfactory results through design of a new technique based on expressing system calibration parameters within the direct-georeferencing equation separately for each target point, and conditioning a group of points to lie on a common surface of a known form.

The camera's focal length is calibrated in-flight by the AT approach with the use of GPS/INS data. As we later show, we found no systematic errors in the LiDAR. Hence, the factory range calibration corresponds to the specified noise level of 0.03 meters.

Operational Challenges

The environment of an in-flight helicopter poses a challenge for GPS/INS integration when the operator tries to determine the sub-decimeter and sub-arc-minute positioning and attitude accuracy, respectively. On one hand, the benign helicopter dynamic has a direct influence on the alignment accuracy of the inertial system. This is because individual systematic errors within the inertial system can be better estimated via GPS/INS integration in the presence of increased horizontal acceleration and rapid change in direction. On the other hand, the vibration level induced by the rotor may be sufficiently intrusive to limit INS short-term orientation precision. Both factors may limit overall system performance when a tactical grade IMU is used with 1°/h gyro drift rates.

To improve the INS alignment accuracy, we adopted GPS-derived azimuth assistance by placing a second antenna on the helicopter's tail. However, we found this approach impractical in some missions and replaced it with periodically repeated flight patterns that take less time.

Rotor-induced vibrations jerk the laser beam and limit the IMU's pointing accuracy. They may also excite unwanted harmonics on the rigid carbon mass holding the GPS antenna. The vibration amplitude can be strong enough to hamper GPS velocity (used for aiding the inertial

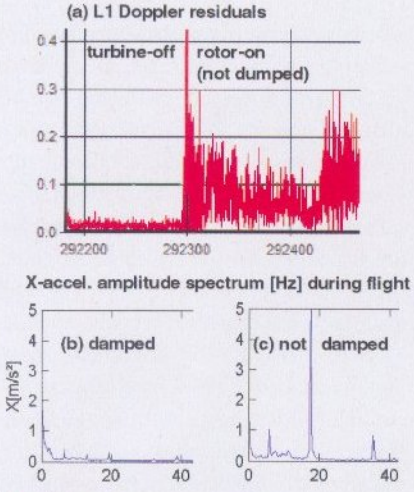

▲ **FIGURE 4** Effect of vibrations on GPS and IMU sensors

system) or, in extreme cases, cause satellite loss of lock (**FIGURE 4**). Fortunately, vibrations can be mitigated by a suspension designed for the sensor head as shown in the IMU data in Figure 4. A similar level of dampening is achieved when the sensor block is handheld by the operator.

Sensor Orientation

The choice of DG or integrated sensor orientation depends on many factors. The rapidity of the former and the robustness of the latter have already been mentioned. A nontrivial and often underestimated decisive factor is the choice of a mapping frame and projection in which orthophotos are delivered. The non-Cartesian character of nationwide projections is causing theoretical and practical distortions within the AT bundle adjustment using GPS/INS observations. A detailed discussion on this subject is beyond the scope of this article. Three mainstream solutions are available when using AT/GPS/INS:

- A set of tight-points (homologous points) is determined first in Cartesian coordinates (for example, tangent-plane projection) and then transformed to the national frame and map projection. Subsequently, the AT is rerun using the new set of coordinates for these points and thus with respect to the national system. The drawback is an introduced distortion to the bundle of image rays.
- Cartesian, typically tangent-plane, projection is used to reconstruct the complete scene and the orthoimage. Subsequently the model is rigorously transformed to the Earth-fixed-Earth-centered (EFEC) frame, and then data transformation and a projection are applied. This is a rigorous approach but it requires relatively laborious 3D orthoimage transformation and resampling.
- Finally, The EOs observed by GPS/INS are modified for the chosen frame and projection prior to the AT input. The AT software can then be run only once and the orthoimages are generated directly in the desired system of coordinates. This approach is fast but not rigorous for the same reason as the first solution. Further approximations are usually taken in the transformation of the camera observed attitude.

The generation of the laser point cloud and the subsequent derivation of a DSM/DTM do not escape the data-projection problem. Here, either of approaches two or three is applicable, although the point-to-point transformation of the DTM usually requires no additional resampling. Height corrections due to geoid apply in all cases.

The following evaluation presents the system's absolute accuracy at discrete points determined on the images. A test field with 25 ground control points (GCPs) was repeatedly used for this purpose. The scale of the images taken within a few strips varied from 1:9000 to 1:11,000, and the accuracy of GCPs (used also as checkpoints) was ~0.02 meters. Because some GCPs were not specially signalized, the measurement of their image coordinates may introduce an additional error of 4 to 8 micrometers (3 to 8 centimeters in the object space).

TABLE 1 compares indirect (AT), integrated sensor orientation and DG approaches to photogrammetric mapping in terms of constraints and empirically estimated accuracy. The RMS values for the DG are slightly higher than those for the indirect or integrated approach, but still remain at decimeter level.

Therefore, the price to pay when adopting DG is not necessary in reduced accuracy but rather in lower reliability and limited quality control. On the other hand, adopt-

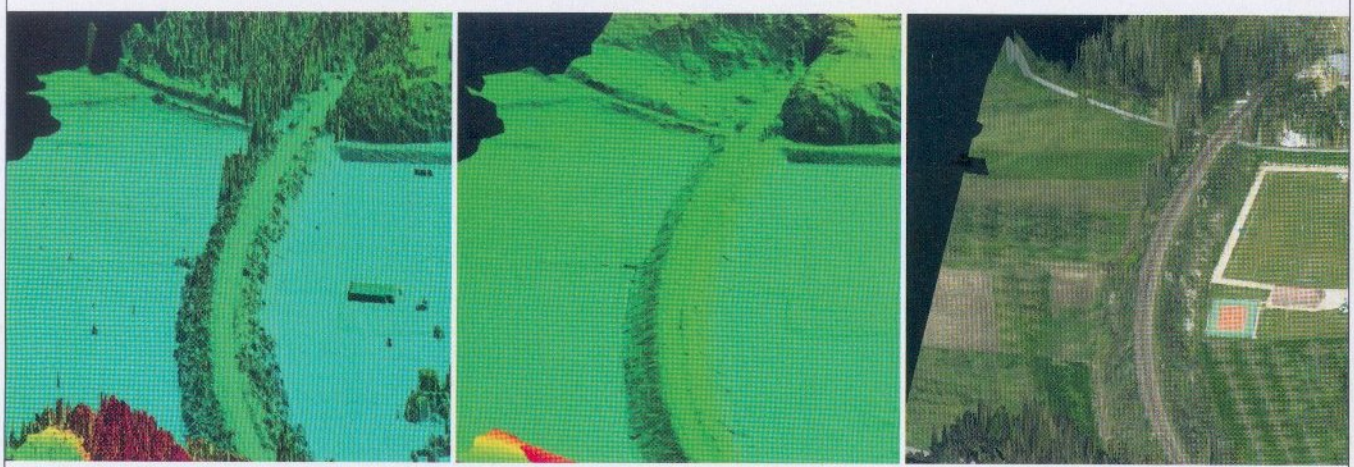

▲ **FIGURE 5** Corridor mapping of a railroad showing three distinct mapping products for better management: (left) digital surface model; (middle) digital terrain model; (right) orthophoto

TABLE 1 Mapping accuracy vs. different approaches.

Method	Constrains		RMS at GCPs [cm] application field		
	GCP	Block	s0 [m]	X,Y	Z
AT	_	_	2	4	4
AT/GPS		_	2	9	10
AT/GPS/INS			2	9	10
DG			7	10	14

ing DG will increase the delivery speed and thus productivity.

Surface Determination

The quality of the surface determination depends on the accuracy of the laser measurements, the point density, and the precision of the laser platform's orientation. For terrain modeling one must also consider the terrain obstruction; furthermore, the derivation of a DTM requires the thinning out of the point clouds and the derivation of break lines. Various tests have been performed and a number of projects have been realized. For data processing we used DTM software specially designed for processing laser measurements that offers a variety of filtering and modeling processes and tools for evaluating the resulting data. For additional controls, we injected data into photogrammetric workstations, and control data were determined by GPS and photogrammetric measurements.

To demonstrate the quality of a laser-derived DTM, **FIGURE 6** illustrates a test flight over a football stadium. Several overlapping and crossing lines were flown over the terrain with different characters with a very high point density of up to five points per square meter.

We obtain a purely qualitative precision analysis by deriving a shaded relief and the terrain presentation by contour lines with an interval of up to 10 centimeters and rendering the resultant 3D scenes.

The laser points in general are very dense; therefore post-processing is very important. However, users of a DTM need a minimum of mass points and the determination of break lines. Depending on the roughness of the terrain the optimum point density can be estimated according to various formulas. Reducing DTM density and comparing it to the one obtained using all laser measurements, we obtained the relationship shown in **FIGURE 7**. The DTM accuracy remains constant for point densities between 0.3 meters and one point per 5 square meters for this particular terrain. However, depending on the soil cover, the initial laser sampling rate must be much higher. To remain on the safe side, it should be five to ten times higher than the finally derived point density.

The most thorough control is achieved by control points; field measurements (GPS points) are ideal because of their high ac-

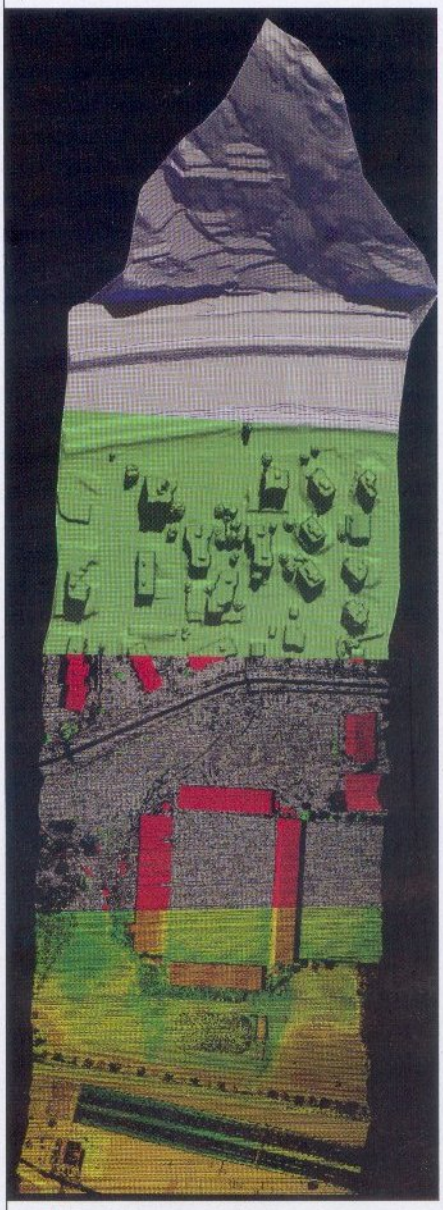

▲ **FIGURE 6** Laser data processing stages from bottom up: 1. color coded laser point cloud, 2. classified points (gray = ground, red = building, green = vegetation), 3. DSM shaded relief (light green), 4. DTM with contour lines.

TABLE 2 Laser mapping accuracy as a function of terrain homogeneity

Surface	Accuracy-RMS [m] relative	absolute
Road	0.03	0.06
Snow	0.06	0.10
Prairie	0.05	0.09
Vegetation	0.09	0.14

curacy. However, these points should be representative and should also model problematic areas. To avoid the uncertainty related to identifying individual laser reflectance spots in the terrain, we mainly work with comparing dense profiles derived from laser and photogrammetric measurements.

TABLE 2 shows the synthesis of such comparison over several profiles over different surfaces. The absolute precision varies from six to 14 centimeters depending on soil character. The higher the vegetation the lower the certitude in the laser last-echo return with respect to actual terrain. The relative precision (noise) within individual strips varies from 3 centimeters on road surfaces to 9 centimeters in dense vegetation. Note that the accuracy of the control data is also on the order of 3 centimeters.

Future Work

The developed system is now used in practice and we plan to focus on faster delivery of the final mapping product, with rapid quality data assessment. This means to determine, as fast as possible, whether a surveying campaign has met client requirements in terms of data precision and resolution. If this goal is reached during the flight, re-flight costs can be avoided. Additional processing onboard the helicopter may create new monitoring applications close to real-time. Finally, rigorous handling of system calibration procedures and adjustment of overlapping laser strip will remain challenging research topics.

Manufacturers

The current HELIMAP configuration uses **Javad** *Lexon-GD* L1/L2 GPS receiver with Javad *AvAnt* antenna *(www.javad.com)*; *LMS-Q240(i)-60* airborne scanner from **Riegl Laser Management Systems** *(www.riegl.co.at)*; a **Hasselblad** *H1* digital camera *(www.hasselblad.com)*; **Imacon** *Ixpress 132C* digital back *(www.imacon.com)*; **Litton** *LN200/A1* inertial navigation system *(www.nsd.es.northropgrumman.com)* with IMU data interface from VNR Electronique *(www.vnrsa.ch)*; *TerraScan* laser point clouds processing package from **TerraSolid** *(www.terrasolid.com)*; Terra Scan DTM software; and *Waypoint GrafNav* GPS post-processing software from **NovAtel** *(www.novatel.com)*.

JAN SKALOUD is a senior scientist and lecturer at the Swiss Federal Institute of Technology Lausanne (EPFL) in Switzerland. He holds a Ph.D. and M.Sc. in Geomatics Engineering from the University of Calgary and Diploma Ing. degree from The Czech Technical University in Prague.

JULIEN VALLET graduated from EPFL with M.Sc. and Ph.D. in photogrammetry and currently directs airborne operation at Ulrich, Wiesmann+Rolle AG SA in Wollerau, Switzerland.

KRISTIAN KELLER is a scientist at the Danish National Space Centre. He has a master's in geodesy.

GRÉGORY VEYSSIÈRE is a visiting research fellow at EPFL.

OTTO KÖLBL is a professor and directs the laboratory of photogrammetry at EPFL.

PHILIPP SCHAER is thanked for his help in producing figures.

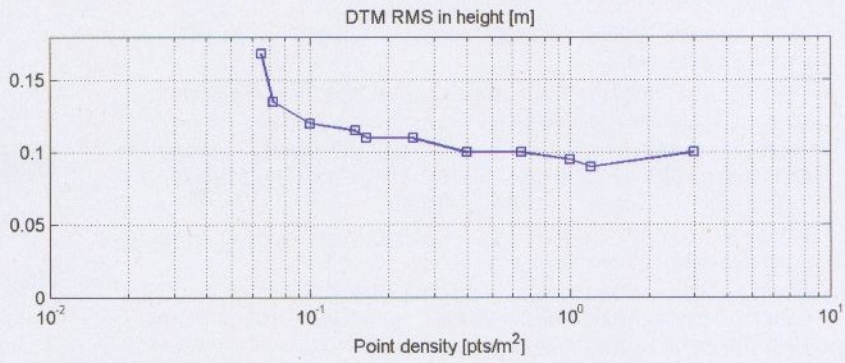

▲ **FIGURE 7** Vertical DTM accuracy as a function of grid spacing (=sampling density).